JOURNAL OF CATALYSIS 157, 656–664 (1995)

Tracer Exchange and Catalytic Reaction in Single-File Systems

Christian Rödenbeck, Jörg Kärger,[1] and Karsten Hahn

Fakultät für Physik und Geowissenschaften, Universität Leipzig, Linnéstrasse 5, D-04103 Leipzig, Germany

Received April 3, 1995; revised July 11, 1995; accepted July 31, 1995

Using a simple jump model of diffusion, Monte Carlo simulations are applied to determine the rate of tracer exchange and the effectiveness factor of chemical reactions in single-file systems. The influence of the characteristic parameters such as the file length, the jump rates, and the reaction rate are investigated. Particular consideration was dedicated to the temperature dependence of the output rate of the chemical reaction. The simulations are compared with the experimentally observed reaction behavior in zeolite L as described in the literature. © 1995 Academic Press, Inc.

1. INTRODUCTION

In contrast to ordinary diffusion, molecular migration in single-file systems is characterized by the impossibility of a mutual interchange of adjacent molecules. The most striking consequence of this situation consists in the proportionality of the mean square displacement of the particles to the *square root* of the observation time (1, 2, 3):

$$\langle r^2(t)\rangle = 2F\sqrt{t}. \qquad [1]$$

Using a simple jump model, the *single-file mobility factor* F may be shown to be given by the relation

$$F = l^2 \frac{1-\Theta}{\Theta} \frac{1}{\sqrt{2\pi\tau}}, \qquad [2]$$

with l, τ, and Θ denoting, respectively, the distance of adjacent sites, the mean time between successive jump attempts, and the mean site occupancy (1, 2, 3). Equation [1] is the analogue of Einstein's equation

$$\langle r^2(t)\rangle = 2Dt \qquad [3]$$

for normal one-dimensional diffusion. Within a simple jump model, the self-diffusivity D, defined by this relation, can be expressed in terms of the jump length l and the mean time τ between successive (uncorrelated) jumps by the equation

$$D = \frac{l^2}{2\tau}. \qquad [4]$$

Due to correlations between the displacements of the individual particles, processes involving single-file diffusion are much more complicated than those accompanied by normal diffusion. That is why they still refuse to be treated by analytical methods except for a few basic results like Eqs. [1] and [2]. Hence one has to resort to numerical simulations.

Two interconnected features dealt with for pore networks in Refs. (4, 5, 6, 7) and, in a preliminary study, for single-file systems in Ref. (3), were investigated in more detail, namely tracer exchange and catalytic reaction. In both cases, the set of primary parameters (jump and reaction rates) was reduced to a set of dimensionless parameters which appeared to correspond best to the structure of the respective problem. The model and the algorithm for the present calculations are basically the same as those used in Ref. (3), although they are expanded and refined in order to allow the investigation of a greater variety of parameters and to avoid some numerical difficulties.

2. TRACER EXCHANGE

2.1. Model

The simulations are based on the following simple model. The single-file channel consists of N sites. Each site is occupied by a particle with probability Θ, the *mean site occupancy*. On average, once in time τ a particle acquires an energy high enough to attempt to jump to the neighbour site, either to the right or to the left. It actually jumps if this site is vacant, otherwise it remains at its place. Hence, the jump rate from a given site to a particular adjacent one is

$$S = \frac{1}{2\tau}\Theta(1-\Theta). \qquad [5]$$

[1] To whom correspondence should be addressed.

0021-9517/95 $12.00

With the rate α (i.e., in the time interval dt with probability αdt) a particle from the surrounding gas phase attempts to occupy a given one of the two marginal sites. It succeeds if this site is vacant. This means an adsorption rate of

$$A = \alpha \cdot (1 - \Theta) \qquad [6]$$

on either of the marginal sites. Molecular desorption from a marginal site is assumed to be activated with the rate ε, provided that the considered marginal site is occupied. This leads to a desorption rate

$$E = \varepsilon \cdot \Theta \qquad [7]$$

from either of the marginal sites. The adsorption/desorption processes at the left and the right margin take place independently from each other. The system is in dynamic *sorption equilibrium*, i.e., the average number of particles occupying the channel is constant. This implies that the rates of molecular adsorption and desorption are equal, i.e.,

$$A = E, \qquad [8]$$

whence, via Eqs. [6] and [7],

$$\Theta = \frac{1}{1 + \varepsilon/\alpha}. \qquad [9]$$

Obviously, the occupancy is determined exclusively by the ratio ε/α, which we introduce as a first dimensionless parameter v. Equation [9] is nothing else than the Langmuir isotherm, if the dimensionless variable $v = \varepsilon/\alpha$ is replaced by the common expression $1/ap$, with a and p denoting, respectively, the Henry constant and the pressure. Rearranging Eq. [9] one has

$$v = \frac{\varepsilon}{\alpha} = \frac{1 - \Theta}{\Theta}. \qquad [10]$$

It is interesting to note that v exhibits the same concentration dependence as the mobility factor F (cf. Eq. [2]), though both quantities refer to different processes in the single-file system, viz. the intracrystalline diffusion (F) and the particle exchange at the margin (v).

A second dimensionless parameter, w, can be introduced as the ratio of the jump rates at the margin and in the interior of the file. Using Eqs. [5]–[7], this parameter may be represented in different ways:

$$\begin{aligned} w &= \frac{A}{S} = \frac{2\alpha\tau}{\Theta} \\ &= \frac{E}{S} = \frac{2\varepsilon\tau}{1 - \Theta} \\ &= 2(\alpha + \varepsilon)\tau. \end{aligned} \qquad [11]$$

It can also be understood as a measure of how fast the marginal sites lose the memory of their occupation after any jump to or from them. The case $w = \infty$, in particular, means that a marginal site will have forgotten its current occupation immediately. The quantity $wN = NA/S$ coincides with the Biot number, being a measure of the ratio of the molecular exchange rates at the boundary (representing the influence of possible surface mass-transfer resistances) and between the center and the boundary in the case of normal diffusion.

At time $t = 0$, let all particles in the file be labelled as tracers. As a consequence of the exchange processes they will be replaced by the unlabelled particles of the gas phase. The microdynamic properties of the labelled and unlabelled particles are completely the same. $\gamma = \gamma(t)$ represents the relative amount of labelled particles that have left the file. The *tracer exchange curve* thus starts at $\gamma(t = 0) = 0$ and approaches more or less rapidly $\gamma(t \to \infty) = 1$. A measure of the rate of the tracer exchange is given by the *intracrystalline mean lifetime*

$$\tau_{\text{intra}} = \int_0^\infty (1 - \gamma)\, dt. \qquad [12]$$

2.2. Algorithm

There are several possible ways to translate the model into computer algorithms, and they differ from a practical and numerical point of view. The one chosen for the present simulations divides the time scale into elementary steps of length $\tau/(N - 1)$. For each step the intracrystalline diffusion is simulated in the following way:

(i) a pair of adjacent sites is selected randomly for a jump attempt;

(ii) the direction of the jump attempt is selected randomly;

(iii) if the selected jump is directed from an occupied to a vacant site, it is carried out.

In the case of finite exchange rates α and ε at the margin, the simulation continues as follows:

(iv) if the left marginal site is vacant, it becomes occupied by an unlabelled particle with probability $\alpha\tau/(N - 1)$; if it is occupied, it becomes free with probability $\varepsilon\tau/(N - 1)$;

(v) the same is done with the right marginal site.

This works only if the probabilities involved are much less than 1, because otherwise rendering the time discrete would lead to erroneous results (8). For infinite exchange rates, $w = \infty$, steps (iv) and (v) are carried out by a special algorithm, namely,

(iv) independently of the current occupation, the left marginal site becomes occupied with an unlabelled particle

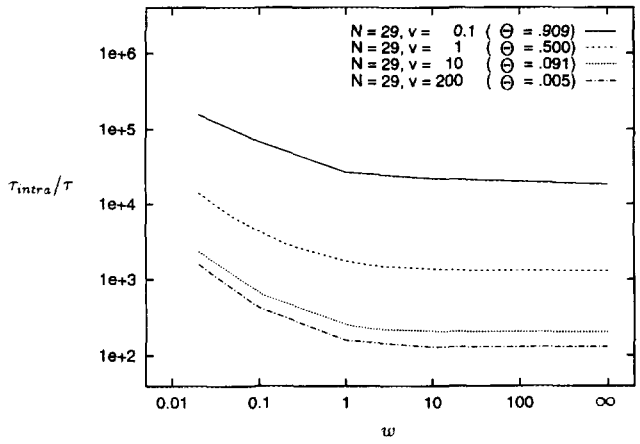

FIG. 1. Dependence of τ_{intra}/τ on the ratio w between the molecular jump rates at the margin and within the file. The different curves correspond to different occupancies, expressed in terms of the ratio v between the rates of emission and adsorption attempts via Eq. [9]. The curve for $v = 200$ (almost empty file) approximates the case of normal diffusion.

with probability Θ or becomes vacant with probability $1 - \Theta$,

(v) likewise the right margin.

The calculated tracer exchange curves are averages over 1000 equal systems. The pseudo-random numbers used in the simulations were generated using a sophisticated algorithm by Marsaglia (9); more simple random number generators sometimes yielded rather strange results and had to be abandoned (8).

The variable τ_{intra} was calculated by numerical integration of the tracer exchange curves. In cases where the exchange time was too long, the curves could not be calculated completely. In these cases, τ_{intra} was determined by extrapolation, taking advantage of the fact that the tracer exchange curves were found to exhibit essentially the same shape.

2.3. *Results*

Since the primary parameters α, ε, and Θ can be expressed in terms of v and w (see Eqs. [9], [10], [11]), the intracrystalline mean lifetime τ_{intra} was investigated in terms of the dimensionless parameters N, v, and w. The mean jump time τ was taken as the unit of the time scale.

Figure 1 shows the dependence of τ_{intra} on the rate of particle exchange at the margin in a log–log representation. As expected, τ_{intra} decreases with increasing exchange rates. For high values of w, the influence of the processes at the margin becomes more and more unimportant, as indicated by the very small slope of the curve in this region. Therefore, in order to exclude any ambiguity due to possible differences in the boundary conditions when comparing different simulations, in almost all the further calculations we have set $w = \infty$. (Translated to the present notation, in Ref. (3) a value of $w = P/(1 - \Theta)$ with mainly $P = 1$ had been used.)

In the limit $v \to \infty$ the site occupancy Θ approaches 0. Hence, a particle should not be restricted by others any more, i.e., the system should behave according to normal diffusion. Explicit simulations of a normal diffusion system show that a value of $v = 200$ (cf. the lowest curve in Fig. 1) is already a reasonable approximation of this limit. Since there are no significant differences between the curves for different v except for a vertical shift which means a factor to the intracrystalline mean lifetime, the parameter w obviously affects systems of normal diffusion and systems of single-file diffusion (independently of the site occupancy) in essentially the same way.

The dependence of the vertical shift on the site occupancy, expressed in terms of the parameter v, is given in Fig. 2 for $w = \infty$ and two different file lengths. For both file lengths considered, the straight parts of the curves ($v \leq 1$) can be approximated by the relation

$$\tau_{intra}/\tau \propto v^{\mu} \quad \text{with } \mu = -1.1 \ldots -1.2. \qquad [13]$$

The crooked parts represent the transition to normal diffusion as discussed above.

Finally, the dependence on the file length was studied. Figure 3 shows a straight line (solid) for the case $w = \infty$, again indicating a power law. The exponent was fitted to

$$\tau_{intra}/\tau \propto N^{\nu} \quad \text{with } \nu = 3.3 \ldots 3.4. \qquad [14]$$

With decreasing N the influence of the parameter w increases, indicated by the increasing spacings between the

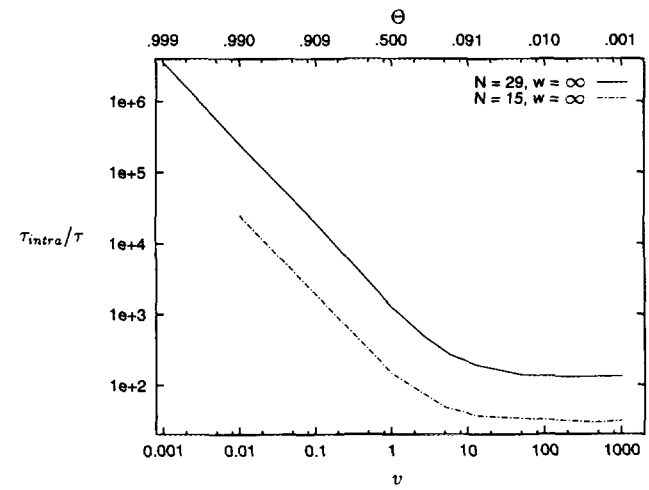

FIG. 2. Dependence of τ_{intra}/τ on the site occupancy, expressed in terms of $v = (1 - \Theta)/\Theta$, for different file lengths.

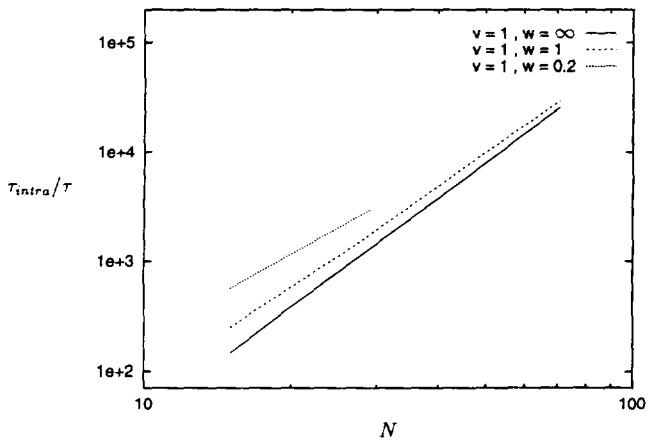

FIG. 3. Dependence of τ_{intra}/τ on the file length for $v = 1$ ($\Theta = 0.5$) and different boundary conditions.

presented curves. Such a behavior is indeed expected because the margin should influence a short file much more than a long one. The simple power law in the case of $w = \infty$ confirms that this boundary condition is a good choice for further simulations.

The shape of the tracer exchange curves proved to depend only slightly on the parameters. The obtained curves lie approximately in the region of the analytical expressions given in Fig. 4. Curve 1 is an exponential function,

$$\gamma_{exp}(t) = 1 - \exp\left(\frac{t}{\tau_{intra}}\right), \qquad [15]$$

which would be the exact solution for a system where the particles *only* have to overcome a marginal barrier. Curve

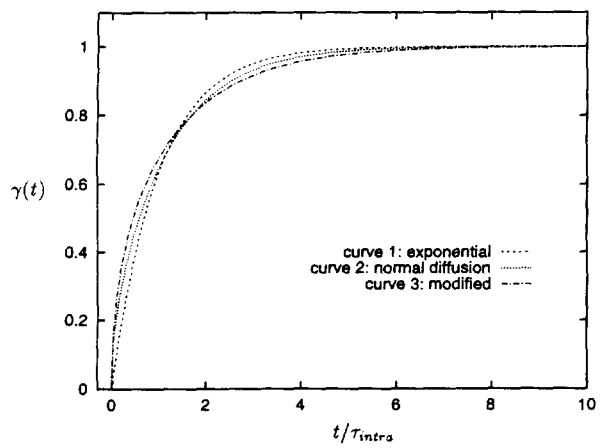

FIG. 4. Analytical approximations for the tracer exchange curve according to Eqs. [15], exponential function, [16], tracer exchange curve of normal diffusion, and [17], modified curve of normal diffusion.

2 represents the tracer exchange curve of normal diffusion (10, 11, 3):

$$\gamma_{n.d.}(t) = 1 - \frac{8}{\pi^2} \sum_{\substack{i=1 \\ \text{odd}}}^{\infty} \frac{1}{i^2} e^{-(\pi^2/12)i^2(t/\tau_{intra,n.d.})}. \qquad [16]$$

Taking the sum over all i yields the modified curve 3:

$$\gamma(t) = 1 - \frac{6}{\pi^2} \sum_{i=1}^{\infty} \frac{1}{i^2} e^{-(\pi^2/15)i^2(t/\tau_{intra})}. \qquad [17]$$

This relation does not represent an exact solution for a particular limiting case. However, the empirically introduced modifications with respect to Eq. [16] proved to allow a reasonably good fit to the simulated curves for a certain range of the parameters.

The dependence of the shape of the simulated curves on the parameters v and w may be systematized in the following way:

- For very large values of the parameter v one expects a behavior approximating normal diffusion. If, in this case, the parameter w is 1 or larger, the simulated tracer exchange curves indeed coincide with curve 2. With decreasing w, i.e., an increasing barrier at the margin, the curves more and more approach the exponential relation curve 1.
- Fixing now $w = 1$ and lowering v, the curves change from the shape of curve 2, moving in the opposite direction, reaching the shape of curve 3 at approximately $v = 1$, and changing further beyond curve 3.
- If finally the parameter v is fixed at a small value and the parameter w is decreased, the shape of the curve changes again towards curve 1, similar to the case of large v described above.

In the case of normal one-dimensional diffusion, the dependence of the intracrystalline mean lifetime on the characteristic parameters of the system under study, viz. the length

$$L = Nl \qquad [18]$$

of the channel and the diffusivity D, may be deduced straightforwardly by realizing that the tracer exchange curve, being dimensionless, can in turn depend on dimensionless quantities only. The only way in which the observation time t may be transferred into a dimensionless quantity is by using the notation tD/L^2. Consequently, the tracer exchange curve must be a unique function of this quantity tD/L^2, and via Eq. [12] one easily finds that

$$\tau_{intra,n.d.} \propto L^2 D^{-1} \propto N^2 \tau, \qquad [19]$$

where the second proportionality follows from Eqs. [18]

and [4]. A straightforward solution of the differential equation of the diffusion with a vanishing concentration at the margin as the boundary condition yields the well-known result (10, 11, 3)

$$\tau_{\text{intra,n.d.}}/\tau = \frac{N^2}{6}. \qquad [20]$$

In the case of single-file diffusion, the same reasoning would lead to the relation $\tau_{\text{intra}} \propto N^4F^{-2} \propto N^4v^{-2}$, where the second proportionality results from the coinciding occupancy dependence of v and F as provided by Eqs. [10] and [2]. While the thus obtained proportionality of the intracrystalline mean lifetime to the fourth power of the file length (which in fact was intuitively implied in Ref. (3)) is not too different from the result of the present simulations (cf. Eq. [14]), the deviation in the dependence on the mobility factor is rather pronounced (cf. Eq. [13]). This apparent discrepancy may be explained by realizing that in consequence of the long-scale correlation the tracer exchange behavior in single-file systems cannot be represented in terms of the mobility factor only. In fact, this correlation affects any pair of particles. Such a correlation does not exist in the case of normal diffusion so that the failure of the simple scaling argument in single-file systems is not unexpected.

The analytical confirmation of the relations [13] and [14] and the derivation of a universal expression for the tracer exchange curve, so far deduced on the basis of the present Monte Carlo simulations, is a real challange for future work.

3. REACTION

3.1. Model

Now the model of the single-file system with particle exchange, which was controlled by the parameters N, v, and w, is expanded by considering an irreversible monomolecular chemical reaction taking place on the individual sites. The reactant molecules which have been adsorbed from the gas phase are converted into product molecules which leave the file by desorption. For simplicity it is assumed that reactant and product molecules have equal transport properties and that desorbed product molecules are never adsorbed again.

Let the *intrinsic reactivity* be k; thus the fraction of molecules reacting during the mean jump time of the diffusion is given by the dimensionless parameter

$$\kappa = k \cdot \tau. \qquad [21]$$

The actual output of product molecules under *reaction equilibrium*, however, is reduced by the diffusion, because

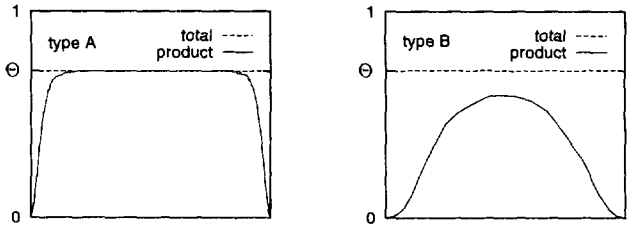

FIG. 5. Two types of profiles of the product concentration and the total concentration.

the reaction can only proceed if the product is replaced by a reactant. Since only sites occupied by a reactant molecule can contribute to the reaction, one has for the *output rate per site*

$$k_{\text{output}} = \overline{\Theta}_{\text{reactant}} \cdot k, \qquad [22]$$

where $\overline{\Theta}_{\text{reactant}}$ denotes the mean site occupancy of reactant molecules. If the site occupancy of product molecules and the total site occupancy are plotted against the position of the site in the file (see Fig. 5), $\overline{\Theta}_{\text{reactant}}$ is proportional to the area between these two concentration profiles. The *effectiveness factor* η is defined as (10, 12, 13, 14)

$$\eta = \overline{\Theta}_{\text{reactant}}/\Theta \qquad [23]$$

and represents the ratio between the actual output of product molecules and the value which would be attained if the molecules were instantaneously replaced by reactant molecules after their reaction.

As in most of the calculations of τ_{intra} in the previous section, the boundary condition was chosen to be $w = \infty$, i.e., the exchange rates at the margin were assumed to be infinitely fast. This means that a product molecule formed at one of the marginal sites will be desorbed immediately.

3.2. Algorithm

Each elementary time step of the algorithm in the previous section is now supplemented by the following procedure:

(vi) one of the sites, except one of the two marginal sites, is chosen randomly for reaction;

(vii) if the site is occupied by a reactant molecule, this is replaced by a product molecule with probability $\kappa(N-2)/(N-1)$.

Since each site is selected $N-1$ times per τ with probability $1/(N-2)$, it will react with probability κ per time τ in agreement with Eq. [21], provided the probability $\kappa/(N-1)$ for the reaction per elementary step is small in comparison to 1 (otherwise the error in consequence of rendering the time discrete becomes too large (8)).

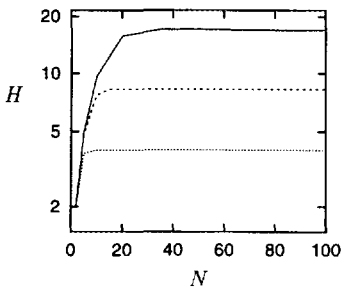

FIG. 6. $H = \eta N$ as a function of N for $v = 1.21$ and $\kappa = 1.1 \cdot 10^{-3}$, $1.1 \cdot 10^{-2}$, or $1.2 \cdot 10^{-1}$, (from top to bottom), respectively.

The calculated values of η are time averages after the system has reached the reaction equilibrium.

3.3. Results

With $w = \infty$ there are three parameters concerned: N, v, and κ. At first N was fixed to 29. This is very small in comparison with the much more realistic estimate of 2000 (3) but was chosen for the sake of computation time, which is always a serious problem in simulations. The effectiveness factor η was simulated for the points of a grid in the (v, κ)-plane with log axes.

It turned out that there are two types of concentration profiles of the product molecules, labelled A and B, respectively, in Fig. 5. When N was increased, profiles of type A retained the shape of their flanks, only the centrepiece became longer. In contrast, profiles of type B changed over into type A for sufficiently large N. Since the effectiveness factor η may be represented as the ratio between the area between the two profiles, which remains constant in the case of type A, and the total area below Θ, which is proportional to N, it is convenient to introduce the quantity

$$H = \eta N, \qquad [24]$$

which is independent of N as long as the profile is of type A. This condition is found to be easily fulfilled for all the considered points in the (v, κ)-plane with values for N never exceeding 2000. Figure 6 shows the complete dependence of H on N for three examples with different values of κ. One may conclude that, under the assumption of N being of the order of 2000, only profiles of type A will occur, and one has

$$\eta = \eta(N) \propto \frac{1}{N}. \qquad [25]$$

This relation expresses the dramatic reduction of the effective reactivity in single-file systems due to transport inhibition, which has already been discussed in Ref. (3).

On the basis of these considerations, the simulations were repeated with N chosen large enough to ensure a profile of type A, a useful rule-of-thumb being $N \gg 4 \cdot H$. The upper part of Fig. 7 shows the values of H over v for different κ in a log–log representation. In the lower part, the same data are represented in a different way; the lines connect all points of the (v, κ)-plane with equal H, thus forming the iso-lines of the effectiveness factor. One decade of H is divided logarithmically into 6 iso-lines, i.e., the transition from one iso-line to the adjacent one means a factor of $\sqrt[6]{10}$ to H. This representation is of special relevance for the discussion of the temperature dependence below. Since the iso-lines are almost parallel in a broad region of the parameter plane, the slope of log H is nearly uniform, becoming slightly steeper for large values of H, as indicated by the narrower spacings between the lines.

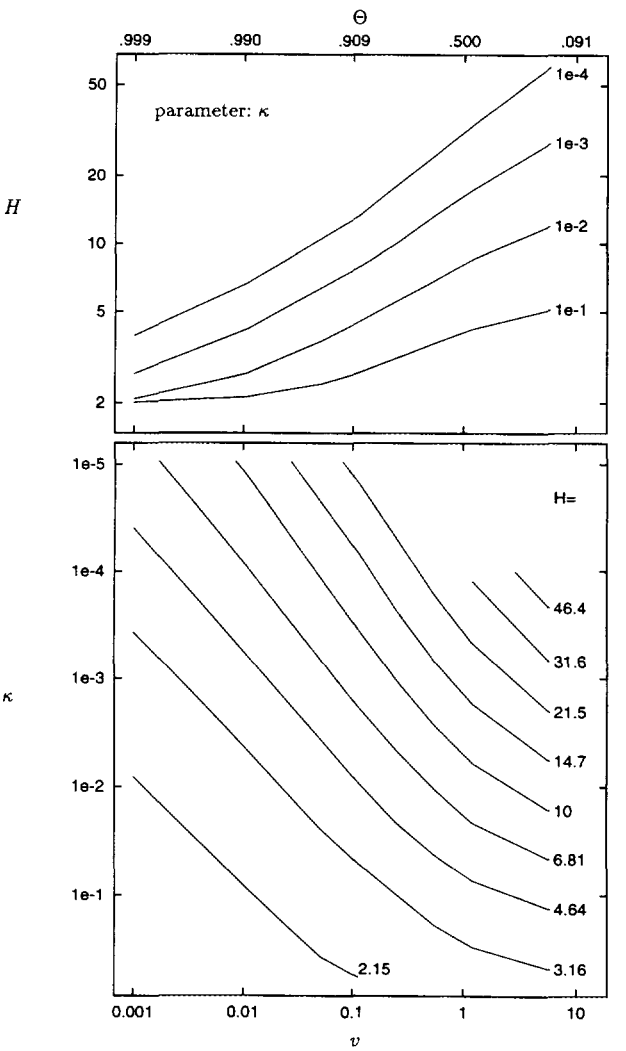

FIG. 7. $H = \eta N$ as a function of $v = (1 - \Theta)/\Theta$ for different κ (above) and as iso-lines (below).

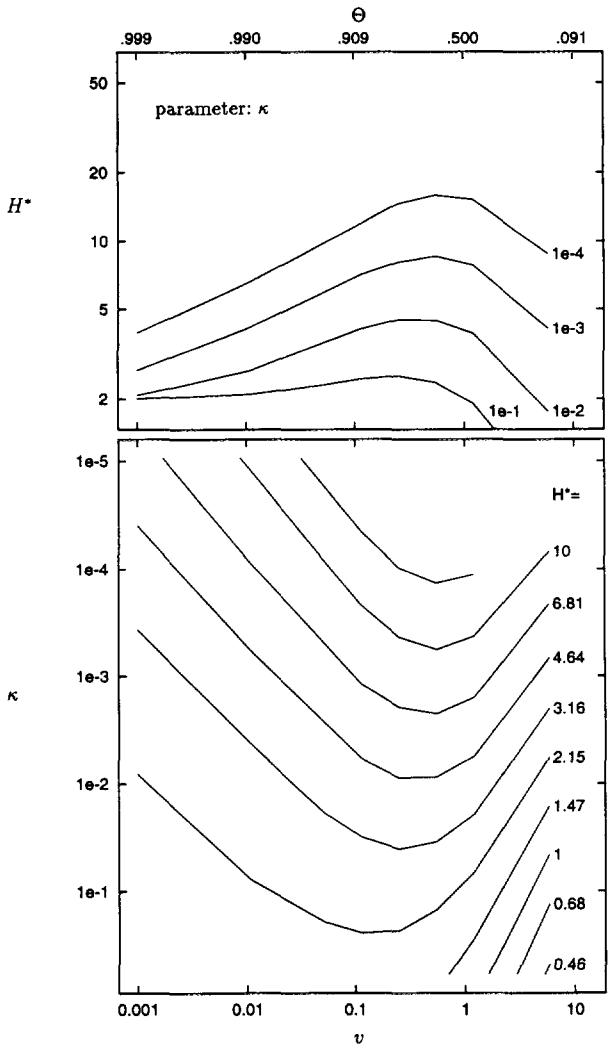

FIG. 8. $H^* = \eta N\Theta$ as a function of $\upsilon = (1 - \Theta)/\Theta$ for different κ (above) and as iso-lines (below).

Finally, in order to obtain the effective output rate of the reaction, the quantity

$$H^* = H \cdot \Theta = \eta N\Theta \qquad [26]$$

was calculated. This quantity can be interpreted as the mean number per channel of sites where conversions actually occur. Due to Eqs. [22], [23], and [26] one has for the *output rate per channel*

$$K = N \cdot k_{\text{output}} = H^* \cdot k. \qquad [27]$$

Note that this quantity is, as are H and H^*, independent of N for sufficiently large N.

Figure 8 shows H^*, again as a function of υ and as iso-lines. For fixed κ, one has a value of υ or Θ, respectively, where H^* has a maximum. This value of Θ increases slightly with κ from $\Theta \approx 0.6$ at $\kappa = 10^{-4}$ to $\Theta \approx 0.8$ at $\kappa = 10^{-1}$.

3.4. Temperature Dependence

Since the primary parameters of the reaction are rates of activated processes they can be assumed to depend on temperature according to an Arrhenius law,

$$\frac{1}{\tau(T)} \propto e^{-E_\tau/RT} \qquad [28]$$

$$\alpha(T) \propto e^{-E_\alpha/RT} \qquad [29]$$

$$\varepsilon(T) \propto e^{-E_\varepsilon/RT} \qquad [30]$$

$$k(T) \propto e^{-E_k/RT}, \qquad [31]$$

with the thermal energy RT and the activation energies E_τ, E_α, E_ε, and E_k. From Eqs. [21] and [10] one has for the activation energies of the dimensionless parameters

$$E_\kappa = E_k - E_\tau \qquad [32]$$

$$E_\upsilon = E_\varepsilon - E_\alpha. \qquad [33]$$

If the activation energy of H^* is known one can calculate the activation energy of K on the basis of Eq. [27]:

$$E_K = E_{H^*} + E_k. \qquad [34]$$

Since the (υ, κ)-plane in the lower parts of Figs. 7 and 8 has log axes, all points $(\upsilon(T), \kappa(T))$ for a variable temperature lie on a straight line which passes the point $(\upsilon(T_0), \kappa(T_0))$ for a given starting temperature T_0 and has a slope that is determined by the ratio E_υ/E_κ. Any given temperature interval corresponds to a certain section of this line, the length of which is proportional to $\sqrt{E_\upsilon^2 + E_\kappa^2}$. By differentiation along the direction of this line one can calculate the activation energy of H^*:

$$E_{H^*} = \frac{\partial \log H^*}{\partial \log \upsilon} E_\upsilon + \frac{\partial \log H^*}{\partial \log \kappa} E_\kappa. \qquad [35]$$

In regions where the iso-lines are approximately parallel and equidistant one can obtain an estimate of E_{H^*} by graphical means. By way of example, Fig. 9 gives the iso-lines of H^* again and a straight line (dashed) with temperature labels, which corresponds to the values (example 1) $\upsilon(T_0) = 0.011$, $\kappa(T_0) = 0.0011$, $RT_0 = 4$ kJ/mol ($T_0 \approx 480$ K), $E_\upsilon = 60$ kJ/mol, and $E_\kappa = 180$ kJ/mol. From this diagram one can read $\Delta \log \upsilon = 0.86$, $\Delta \log \kappa = -0.88$ (lengths of the dotted lines) and $\Delta \log H^* = 1/6$ (step of the iso-lines), which gives $E_{H^*} = -22$ kJ/mol, valid at

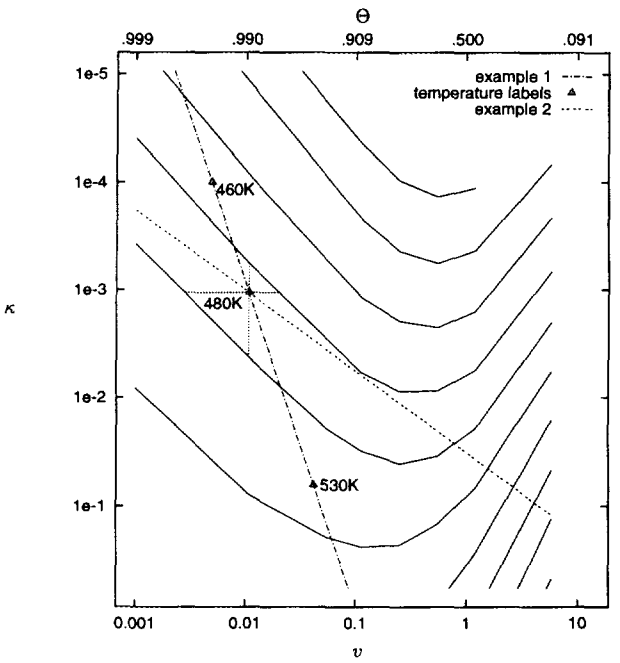

FIG. 9. Examples illustrating the calculation of the activation energy of H^*.

temperatures around T_0. Assuming, e.g., E_τ = 12 kJ/mol, one finally has E_K = 170 kJ/mol.

In example 2 with E_v = 80 kJ/mol and E_κ = 60 kJ/mol one obtains E_{H^*} = 4 kJ/mol. With this positive value one has an effective activation energy of the reaction of E_K = 76 kJ/mol which notably *exceeds* the activation energy of the intrinsic reaction, E_k = 72 kJ/mol. This finding is in striking contrast to the well-known situation under the influence of normal diffusion, where transport control always *lowers* the effective activation energy, ultimately (for negligibly small activation energies of intracrystalline diffusion) to half the activation energy of the intrinsic reaction (10). Although catalytic reactions in single-file systems are, by their very nature strongly transport controlled, due to the inhibition of mutual passage of the individual molecules, the transport rate, in contrast to systems with normal diffusion, depends on concentration, which in turn depends on temperature. Therefore, in the case of sufficiently large values of E_v (corresponding to large heats of adsorption) the concentration dependent factor $(1 - \Theta)/\Theta = v$ in Eq. [2] will increase with increasing temperature so that the molecular exchange rate between the interior of the single-file system and the surrounding gas phase can increase even more strongly than the intrinsic reactivity, which leads to an effective activation energy of the reaction larger than the activation energy of the intrinsic reaction. In example 2 such a situation is in fact considered.

With the advent of a multitude of zeolite catalysts with one-dimensional channel systems, the first extensive experimental studies of catalytic reactions in systems which may be supposed to be of the single-file type have begun to appear in the literature (15, 16, 17, 18). Interestingly enough, in a systematic study of neopentane conversion catalyzed by palladium-containing zeolites (15) the effective activation energy in zeolite L was found to be much larger than in zeolite Y (and larger than the activation energy of the intrinsic reaction), although transport control in the single-file type zeolite L must clearly be much more pronounced than in the three-dimensional pore network of zeolite Y. In Ref. (15) this behavior has been intuitively correlated with the particular situation in single-file systems. The present simulations confirm that in single-file systems such an inversion of the influence of transport control on the effective activation energy of catalytic reactions may in fact occur.

4. CONCLUSION

Tracer exchange and catalytic reactions in single-file systems have been studied systematically by Monte Carlo simulations covering a large range of values for the characteristic parameters of the system. For the first time the influence of the boundary conditions in single-file systems has been considered quantitatively and scaling laws for the dependence of the tracer exchange times on the file length and on the file occupancy have been derived. Considering the intracrystalline irreversible monomolecular conversion between two molecular species of identical adsorption and transport properties, typical features of catalytic reactions in single-file systems are traced. Representations of the effective reaction rates as a function of the site occupancy and of the intrinsic reactivity are given, covering five orders of magnitude for the corresponding dimensionless parameters. Depending on the activation energies of these parameters, the effective activation energy of the reaction may be even larger than the activation energy of the intrinsic reaction. Such a situation is in striking contrast to the behavior of systems undergoing normal diffusion and appears to be a special feature of single-file systems. Conversion studies with neopentane in the single-file type zeolite L, presented in the literature, do in fact comply with such a behavior.

APPENDIX: NOMENCLATURE

Arabic

A	adsorption rate
a	Henry constant
D	diffusion coefficient
E	desorption rate
E_G	activation energy of the quantity G
F	single-file mobility factor
k	intrinsic reactivity

k_{output}	output rate per site
K	output rate per channel
l	step length
L	file length
N	number of sites per file
p	pressure
r	displacement
R	gas content
S	intracrystalline jump rate
t	time
T	temperature
T_0	starting temperature
v	dimensionless parameter determining the mean site occupancy
w	dimensionless parameter determining the rate of particle exchange at the margin

Greek

α	rate of adsorption attempts
ε	rate of desorption attempts
$\gamma(t)$	tracer exchange curve
η	effectiveness factor
H	ηN, effectiveness factor times number of sites
H^*	$\eta N\Theta$, mean number of sites active in the reaction
Θ	mean site occupancy
$\overline{\Theta}_{reactant}$	mean site occupancy of reactant molecules
κ	dimensionless parameter determining the fraction of reactant molecules converting during time τ
τ	mean time between succeeding intracrystalline jump attempts
τ_{intra}	intracrystalline mean lifetime
$\tau_{intra,n.d.}$	intracrystalline mean lifetime of normal diffusion

ACKNOWLEDGMENTS

Stimulating discussions with Professors Harry Pfeifer, Wolfgang M. H. Sachtler, and Jens Weitkamp are gratefully acknowledged. We thank one of the referees for helpful comments concerning the correlation of our simulation data with experimentally accessible quantities. We are obliged to the Deutsche Forschungsgemeinschaft (SFB 294) and to the Max-Buchner-Stiftung for financial support.

REFERENCES

1. Fedders, P. A., *Phys. Rev. B* **17,** 40 (1978).
2. van Beijeren, H., Kehr, K. W., and Kutner, R., *Phys. Rev. B* **28,** 5711 (1983).
3. Kärger, J., Petzold, M., Pfeifer, H., Ernst, S., and Weitkamp, J., *J. Catal.* **136,** 283 (1992).
4. Theodorou, D. M., and Wei, J., *J. Catal.* **83,** 205 (1983).
5. Aust, E., Dahlke, K., and Emig, G., *J. Catal.* **115,** 86 (1989).
6. Nelson, P. H., Kaiser, A. B., and Bibby, D. M., *J. Catal.* **127,** 101 (1991).
7. Tsikoyiannis, J. G., and Wei, J., *Chem. Eng. Sci.* **46,** 233 (1991).
8. Rödenbeck, C., Diploma thesis, University of Leipzig, Faculty of Physics and Geophysics, 1995.
9. Marsaglia, G., and Zaman, A., *Statist. Prob. Lett.* **9.1,** 35 (1990).
10. Kärger, J., Ruthven, D. M., "Diffusion in Zeolites and Other Microporous Solids." Wiley-Interscience, New York, 1992.
11. Ruthven, D. M., "Principles of Adsorption and Adsorption Processes." Wiley, New York, 1984.
12. Haag, W. O., Lago, R. M., and Weisz, P. B., *Discuss. Faraday Soc.* **72,** 317 (1982).
13. Garcia, S. F., and Weisz, P. B., *J. Catal.* **144,** 109 (1993).
14. Karge, H. G., and Weitkamp, J., *Chem. Ing. Techn.* **58,** 946 (1986).
15. Karpiński, Z., Ghandi, S. N., Sachtler, W. M. H., *J. Catal.* **141,** 337 (1993).
16. Ernst, S., Weitkamp, J., Martens, J. A., and Jacobs, P. A., *Appl. Catal.* **48,** 137 (1989).
17. Kumar, R., and Ratnasamy, P., *J. Catal.* **116,** 440 (1989).
18. Lei, G.-D., and Sachtler, W. M. H., *J. Catal.* **140,** 601 (1993).